Coherent control of quantum states

Linda Haals

Master's Thesis
LRAP - 319, April 2004

Abstract

In this Master's thesis coherent driving techniques are investigated in order to prepare rare-earth ions in well-defined quantum states. Advantage is taken of the adiabatic[1] passage technique and its robustness against variations of different parameters, in order to create an efficient population transfer between energy states in ions. The work is concentrated on the production of an adiabatic passage, using a laser pulse in the shape of a complex hyperbolic secant function, both in exciting ions at resonance, in a single-shot, as well as in selecting a single-frequency ion group left in the ground state. Thanks to a stabilised laser source in the investigated spectral region, the results have showed very high rates of transfer, which is presented in this report.

[1] A process is in which no heat is gained or lost by the system.

Contents

1 Introduction 7

2 Quantum Computing 9

2.1 Qubits....9

2.2 Quantum logic gates....9

2.3 Preparing a quantum gate in rare-earth ion doped crystals....11

3 Coherent driving of Bloch-vector 15

3.1 Equation of motion in a semi-classical approximation....15

3.2 The Hamiltonian of the atom in interaction with the environment....15

3.3 The Bloch equations....16

3.4 The Bloch-sphere....16

3.5 Rectangular pulse, with fixed amplitude, frequency and phase....17

3.6 Rapid adiabatic passage (RAP)....19

3.5.1 Vectorial picture....19

3.5.2 Complex hyperbolic secant (CHS)....20

4 The experiments 25

4.1 The acousto-optic modulators....25

4.2 Electronics....26

4.3 The set-up....27

4.4 The laser....28

The results of adiabatic passage 33

4.1 Rectangular pulse with fixed amplitude and varying detuning.....34

4.2 Complex hyperbolic secant pulse.....36

5.2.2 Study of the transfer at an increasing power of the writing beam.....37

5.2.3 Selection of a group of ions and transfer to the excited state and back 38

5.2.4 Laser stabilisation.....39

5.2.5 Successive pulses 40

5 Conclusion **43**

Acknowledgements 45

6 References **47**

1 Introduction

Information is sensitive to in what way it is expressed. It can be freely translated from one form to another, which makes it a candidate to play an important role in the world of physics, such as for instance energy and momentum. The combination of information theory and quantum mechanics has led to some exciting new insights in the field of science and the relative new concept of mathematical treatment of information is only dating from the 1920th. As recent as 1994, Shor came up with an algorithm, efficient for a quantum computer to factorise large integers, but meanwhile he addressed a central problem also for a conventional computer.

Building a quantum computer is beyond the abilities of today's technology, but nevertheless, elementary quantum information operations can be implemented and the principles of quantum computing can be carried out and tested in smaller devices. Whithin the research project to which this master thesis is connected, the present challenge is to create isolated groups of rare-earth ions, that can serve as important elements in a quantum computing system based on rare-earth ion doped crystals and also to invent techniques to control these ions to a high presision.

ESQUIRE[2] is a research project within the European Union and this Master thesis has been carried out within the frame of the ESQUIRE project. Research groups in Lund (Sweden), Aarhus (Denmark), Caen and Paris (France) take part in this collaboration. This work took place at Laboratoire Aimé Cotton in Paris, where in particular efficient and robust techniques for population transfer between energy states are developed, which should be viewed as the first step towards the preparation of a atom in a superposition state.

In this report, the first chapter introduces some basic knowledge of quantum computing, followed by a theoretical chapter mathematically describing the physics behind the coherent excitation of an atomic system. In the other chapters, the set-up, instruments and the results of the experiments are discussed. The report is based on recently obtained results, connected to well-known theories. In these latest experiments, with several improvements concerning the equipment, better outcomes have been reached and yet another step in the right direction has been taken.

[2] **E**xperimental realisation of quantum gates and development of **S**calable **QU**antum computer schemes In **R**are-**E**arth-ion-doped inorganic crystals

2 Quantum Computing

As in a classical computer, logical gates operating on bits are the building blocks also of a Quantum Computer (QC). A Quantum Computer uses quantum bits, or qubits, that are constituted of two-level quantum systems, that interact with each other sufficiently to control each other and therefore can serve as elements in quantum logic gates operations. Promising methods suitable to prepare a pure quantum state are ion trapping [1], NMR (Nuclear Magnetic Resonance) [2] and what is focused on in this work, the selection of ions in rare-earth ions doped crystals.

Quantum state entanglement and superposition has been used as a computational resource in the development of the theory of quantum computing, quantum cryptography, teleportation, quantum error correction.

2.2 Qubits

A single qubit can be envisaged as a two-level atom described of a quantum system. A quantum system is expressed in terms of a quantum state, $|\Psi\rangle$. The quantum state is described as a combination of two pure states, called a superposition state:

$$|\Psi\rangle = \alpha|0\rangle + \beta|1\rangle \tag{2.1}$$

where α and β are complex coefficients. The probabilities of finding an atom in one of these states are, respectively, $|\alpha|^2$ and $|\beta|^2$. This is the way of describing a single qubit in a two-dimensional complex vector space, spanned by the orthogonal basis state $|0\rangle$ and $|1\rangle$. Practically, the logical qubits are ions in a crystal, ions that can exist in two different states.

To perform calculations, a complete system with n qubits have to be used, which is said to have n qubits, if it has a Hilbert space of 2^n dimensions and therefore have 2^n orthogonal quantum basis vectors. Yet, to explain the basic functions of quantum computing it will be concentrated on a two-qubit system in this report.

2.3 Quantum logic gates

A quantum computer is manipulated by logic gates. In the classical logic gate, the system is built on a well-defined outcome, either 0 or 1, whereas in quantum computing the system acts linearly between the states $|0\rangle$ and $|1\rangle$.

Generally computer operations require that the value on the bit determines what operation is carried out in another qubit, i.e. a logical operation has to be used. Such logical operation also has to be implemented on the system that is used here.

In this system logical gates are based upon the coupling between qubit ions, that is taking place when by an applied laser pulse one ion is excited which is giving raise to a shift in the transition frequency of the closest situated ions (Figure 1). Thus, whether the ion is resonant with the laser or not, depends on if the neighbour atom exists in the ground state or in the excited state.

The absorption frequency is strongly dependent on the surrounding electric field due to the electric dipole moment of the ions, which will be affected when applying an external electromagnetic field. As an optical transition from the ground state to the excited state is performed in an atom it exhibits a change of dipole moment, which affects the neighbouring ions that will consequently experience a shift in their transition frequency. This is illustrated in Figure 1.

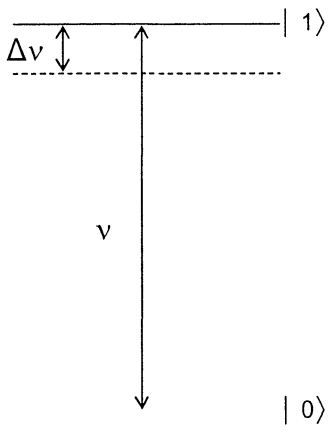

Figure 1. The change in dipole moment, due to excitation, gives raise to a frequency shift, $\Delta\nu$, in the ions close to the excited ion.

The frequency shift of ion *i* due to the interaction with ion *j* is given by [3]:

$$\Delta\nu_{ij} = \frac{(\Delta\mu_i)(\Delta\mu_j)}{4h\varepsilon\varepsilon_0 r_{ij}^3}\left[\left(\hat{\mu}_i \cdot \hat{\mu}_j\right) - 3\left(\hat{\mu}_i \cdot \hat{r}\right)\left(\hat{\mu}_j \cdot \hat{r}\right)\right], \qquad (2.2)$$

where $\Delta\mu = \left|\mu_e - \mu_g\right|$, h is Planck's constant, ε_0 is the permittivity of vacuum and r_{ij} is the distance between the atoms. The parameters $\hat{\mu}$ and $\hat{r}$ are unit vectors along $\left(\mu_e - \mu_g\right)$ and r_{ij}.

An example describing how a controlled NOT-gate (C-NOT-gate) can be implemented in a two-level system, between two arbitrary ions *i* and *j*, is presented in [3] with a scheme illustrated as in Figure 2.

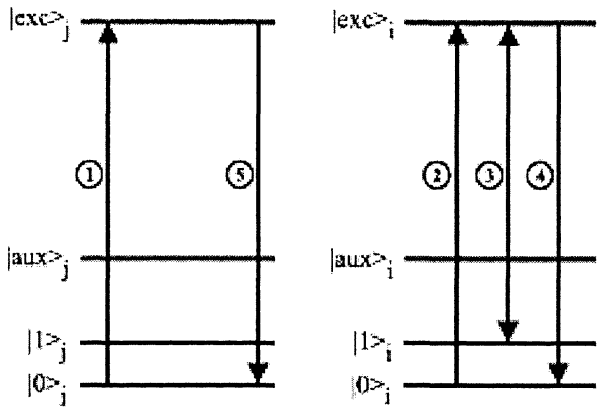

Figure 2. Scheme that shows the most essential steps in producing a controlled NOT-gate. The arrows correspond to the successive pulses and the numbering indicates the time ordering. The level $|\text{aux}\rangle$ illustrates the meta-stable state, which will be discussed further in this report.

The ion *i* is used as the target bit and *j* as the control bit. A laser applies a pulse (1), on the control bit *j*, in resonance with the transition frequency between the ground state, $|0\rangle$ and $|\text{exc}\rangle$, where the latter corresponds to the excited state in this presentation. If the ions are in the $|1\rangle$ state, nothing happens and next step is to apply a pulse (2)-(4) exchanging the population in states, $|0\rangle$ and $|1\rangle$ for the target bit. If the control bit was in its ground state, it will be excited by the pulse (1) causing a shift of all neighboring ions out of their original transition frequency, especially the transition frequency of the ions consisting of the target bit will be shifted. By the following pulse (3), the population transfer of *i* to the state $|\text{exc}\rangle$ will now be possible, and a transfer of the population back to the $|0\rangle$ state by pulse (4) can be carried through. Finally, the pulse (5) is bringing back the control bit to its ground state and canceling out all the shifts of frequency shifts in the target bit. This procedure is equivalent to using the ion *i* is as the control bit and the ion *j* as the target bit.

After having shown that the construction of a C-NOT-gate is possible in these atoms, the most interesting aspect distinguishing a quantum operation and a classical operation, will now be introduced. Qubits existing in the pure states, the ground state $|0\rangle$ or in the excited state, that we from now on will denote $|1\rangle$, have two different outcome possibilities. Either, the control qubit is in the ground state, making possible a transition of the target qubit, from the excited state to the ground state or from the ground to the excited. Or, the control qubit is in its excited state and nothing happens with the target qubit. More interesting is when the qubit is in a superposition between the states $|0\rangle$ and $|1\rangle$, which makes the result slightly more complex. Suppose that the control qubit is in a superposition state and the target

qubit in the $|0\rangle$ state. As a C-NOT operation takes place, putting the qubits in a combination of state as:

$$(|1\rangle+|0\rangle)_{control}\otimes|0\rangle_{target}\rightarrow|1\rangle_{control}\otimes|1\rangle_{target}+|0\rangle_{control}\otimes|0\rangle_{target} \quad (2.3)$$

which can also be written as $|11\rangle+|00\rangle$ in a more compact notation and becomes the new, entangled state of the system. The two qubits are in a non-separable state, meaning that in performing any further operations on the entangled states, it will not be possible to return the qubits into their initial states.

The fact that the quantum C-NOT gate gives a result that is, somewhat a combination of information, is very interesting in, for instance, in the world of research, where enormous amounts of data are to be calculated and analysed. Receiving and treating outputs in this particular way, the comparison between different results can be facilitated and done within a shorter amount of time.

2.4 Preparing a quantum gate in rare-earth ion doped crystals

The C-NOT gate is an important operation in computing. If a creation of such a gate is possible, starting from an atomic quantum state, the performance of a quantum computer will also be reachable. However, first of all we need a greater understanding of the quantum states, how to produce a certain number of qubits and how to control them in a satisfying way. To produce a single qubit with suitable properties has been proved to be very challenging. There are two methods to experimentally create qubits, the ion trap and the NMR that have been successful, except that neither of these methods can scale in to a large number of qubits which is essential for quantum computing. In this report it will only be focused on the concept of rare-earth ions doped in crystals, and why they are good candidates for the creation of quantum bits.

Rare-earth-ions (REI) doped into crystals possess many attractive features, that make them very favourable in the implementation of quantum gates [4]. The rare earth ions have a partially filled inner shell that is shielded from the environment by the outer electrons, resulting in a very narrow homogenous transition line width. For a Eu^{3+}-doped $YAlO_3$ used as a model, the homogenous line width is typically 1 kHz. The imperfections in the host crystal's lattice, give raise to shifts of the transition frequency of the doped ions, which shows how strongly the exact frequency depends on the surrounding electric field. This local field that varies from one position of an ion to another, shifts the ions with different amounts, leading to a large inhomogeneous broadening of their optical transition.

To allow a very large number of consecutive quantum operations without loosing in coherence, a sufficiently long coherence time is necessary. Optical coherence times up to 6.5 ms has been observed in Er^{3+}:YSO in a magnetic field [5]. Another interesting feature is, the relaxation time between the different levels of hyperfine splitting, due to the nuclear quadrupole interaction, which can be up to several

hours or even days. This remarkable combination of long coherence time and an inhomogeneous broadening, which by far exceeds the bandwidth of today's fastest electrical devices has been proved to be an efficient prospect of optical signal processing.

The ESQUIRE project is targeted on showing that RE ions are good candidates for quantum computing and the work required to reach this goal includes the development of techniques for coherent excitation driving of an ensemble of ions, in the qubit preparation and for qubit control [6]. Also growing new crystal materials, specially designed for quantum gate operations, as well as, developing schemes and architectures for REI-crystals, using materials and parameters based on experimental results, are part of the project.

The scheme presented in Figure 2, concerning the production of logic gates, requires an element that has a ground level consisting of several hyperfine levels. Until the time being, experiments have been carried through only on Eu^{3+} and Pr^{3+}, which have a suitable hyperfine level to obtain this kind of scheme [7].

Creating a total population transfer in Eu^{3+} and Pr^{3+} has still not been achieved. Instead this work has focused on a Tm^{3+}-doped crystal, where the ground level does not exhibit a hyperfine-splitting. In the frequency region corresponding to the transition in this system, reliable laser sources have since long been developed. Optical excitation only involves two levels. Then it is not possible to create population inversion, with optical pumping only. A coherent procedure is required, which will be described more thoroughly in the next chapter.

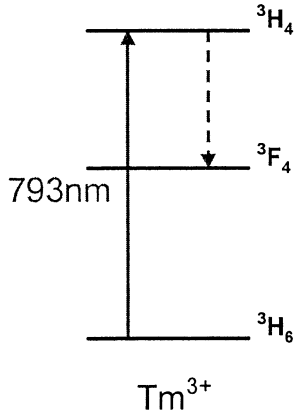

Figure 3. Tm^{3+} with a transition frequency at 793 nm. Separation of the levels $^3H_4$ and $^3H_6$, is suitable for the light source and the frequency modulator available.

If we succeed to control the population transfer and the isolation of a ion group restricted to a narrow frequency region in the inhomogeneous profile in Tm^{3+}, the results will help us to better understand the coherent excitation driving of ions. This result can be applicable on other materials and would be a big step forward on our way towards the controlling of quantum states.

3 Coherent driving of Bloch-vector

A quantum gate is very demanding in terms of the atom excitation control. First of all, atoms should be prepared in a well-specified state and secondly, the operation may require repeated excitation processes, without a too strong accumulation of errors. These conditions which have to be fulfilled are rather new in the context of atom excitation. Indeed, dynamic processes, usually investigated in atomic and molecular physics, do not require such precision. As a consequence, an effort has to be devoted to the excitation scheme design, where the exact amount of superposition has to be controlled. The development of efficient schemes for selective population transfer, such as excitation with laser pulses varying in frequency, rapid adiabatic passage and complex hyperbolic secant pulse have opened new opportunities for laser control of atomic processes, thanks to faster and more efficient processes.

All the techniques concerning total population transfer have one thing in common, the use of coherent laser radiation. With incoherent light the best population transfer that can be achieved is an equalisation of the ground and the excited level, while a coherent source enables a complete transfer to the excited level. In this part it will be investigated how populations can be transferred when using a coherent energy source.

3.2 Equation of motion in a semi-classical approximation

To explain the interaction between the atomic systems, which in this context is conveniently expressed in terms of quantum mechanics, and the classical electromagnetic field, a semi-classical approach is used to envisage the atom-radiation interaction. An atom in an applied electric field is studied, where the interaction dynamics for the coherent excitation is described by the time-dependent Schrödinger equation:

$$ih\frac{d}{dt}|\Psi(t)\rangle = \hat{H}|\Psi(t)\rangle, \tag{3.1}$$

with the wave function, $|\Psi\rangle$.

3.3 The Hamiltonian of the atom in interaction with the environment

Let atoms be prepared in a superposition state:

$$|\Psi\rangle = a|a\rangle + b|b\rangle. \tag{3.2}$$

In the absence of interaction with the environment, such as neighbouring atoms, matrix vibrations etc., the atoms return to their ground state with decay rate, γ_b, whereas, the quantity ab*, reflecting the coherent nature of the superposition state,

is vanishing with decay rate of $\gamma_{ab} = \gamma_b/2$. Elastic interactions with the environment strongly affect the coherence ab*, without modifying γ_b. Due to elastic interaction, $\gamma_{ab} > \gamma_b/2$. A convenient way to account for the system coupling with the environment is to describe the system in terms of the density matrix ρ:

$$\rho = \begin{pmatrix} \rho_{aa} & \rho_{ba}^{*} \\ \rho_{ab} & \rho_{bb} \end{pmatrix}, \tag{3.3}$$

The diagonal terms of the matrix represent the populations of the different states. The off-diagonal elements, ρ_{ba} describe the coherence of the states, between which the atoms are oscillating. The Schrödinger equation can now be evaluated as:

$$i\hbar\frac{d\rho}{dt} = \left[\hat{H},\rho\right] - \left.\frac{d\rho}{dt}\right|_{relaxation}. \tag{3.4}$$

This shows how the populations are related to the value of coherence and the evaluation of coherence is related to the difference in populations, proving that the interaction material-radiation is a mutual coupling between dipole and population.

3.4 The Bloch equations

Based on the hypotheses that the field can be represented classically and the interactions are described in the electric dipole approximation, we can develop the Schrödinger equation into the so-called Bloch-equation, that is expressed as:

$$\begin{aligned} \dot{\rho}_{aa} &= i\left(\frac{\Omega_R e^{i\omega t}}{2} + c.c.\right)\left(\rho_{ba} - \rho_{ab}\right) + \gamma_b\rho_{bb} \\ \dot{\rho}_{bb} &= -\dot{\rho}_{aa} \\ \dot{\rho}_{ab} &= i\left(\frac{\Omega_R e^{i\omega t}}{2} + c.c.\right)\left(\rho_{bb} - \rho_{aa}\right) + \rho_{ab}\left(i\omega_{ab} - \gamma_{ab}\right) \end{aligned} \tag{3.5}$$

where the Rabi frequency Ω_R, associated with the strength of the ion-field interaction, reads as:

$$\Omega_R = \frac{-\mu_{ab}E(t)}{\hbar}. \tag{3.6}$$

We make the transformation:

$$\tilde{\rho}_{ba} = \rho_{ba}e^{-i\omega t} \tag{3.7}$$

and substituting this quantity in Eq. (3.5), we get some rapidly oscillating terms in the form of $e^{\pm 2i\omega t}$. These terms average to zero on the atomic system evolution time scale and we therefore neglect them. This procedure is known as the Rotating Wave Approximation (RWA). Within the frame of this approximation the Bloch equation reads:

$$\begin{cases} \dot{n}_{ab} = i\Omega_R(\tilde{\rho}_{ba} - \tilde{\rho}_{ab}) - \gamma_b(n_{ab} - n_{ab}^{(0)}) \\ \dot{\tilde{\rho}}_{ab} = -\frac{i}{2}\Omega_R n_{ab} + (i\Delta - \gamma_{ab})\tilde{\rho}_{ab} \end{cases} \tag{3.8}$$

where $n_{ab} = \rho_{aa} - \rho_{bb}$ denotes the population density difference, $\Delta = \omega_{ab} - \omega$ stands for the atomic transition and laser frequency difference and $n_{ab}^{(0)}$ represents the population density before excitation.

A geometrical representation of this equation is available in terms of vector precession in a virtual three-dimensional space.

3.5 The Bloch-sphere

Let us define the components of the vector, $\bar{R}(u, v, w)$, known as the Bloch-vector, through the following equations:

$$\begin{aligned} u &= \tilde{\rho}_{ba} + \tilde{\rho}_{ab} \\ v &= i(\tilde{\rho}_{ab} - \tilde{\rho}_{ba}) \\ w &= \tilde{\rho}_{bb} - \tilde{\rho}_{aa} = -n_{ab}. \end{aligned} \tag{3.9}$$

The w-component tells us where the population is. The u- and v-axis are related to the phase coherence of two states. Expressing Eq. (3.5) in terms of these new variables one obtains:

$$\begin{cases} \dot{u} = -\Delta v - \gamma_{ab} u \\ \dot{v} = \Delta u - \Omega_R w - \gamma_{ab} v \\ \dot{w} = \Omega_R v - \gamma_b(w - w^{(0)}) \end{cases} . \tag{3.10}$$

Let us define the vector $\bar{\Omega} = -\Omega_R \bar{e}_u + \Delta \bar{e}_w$. Then Eq. (3.10) takes on the following vectorial form:

$$\frac{d\bar{R}}{dt} = \bar{\Omega} \times \bar{R} + \text{relaxation terms} \quad . \tag{3.11}$$

This equation expresses the precession of $\bar{R}(u, v, w)$ around the $\bar{\Omega}$-vector at the rate of: $\sqrt{\Omega_R^2 + \Delta^2}$. This is illustrated in Figure 4. The 3D-space where the Bloch vector evolves is not related to the physical space. It should be noticed that in the absence of field, the Bloch vector precesses at rate Δ around the vertical axis. Since $\bar{\Omega}$ has no component along v, the field does not affect the Bloch-vector, when this vector is directed along the u-axis whereas the effect on the Bloch-vector is the strongest when the field is aligned along the v-axis.

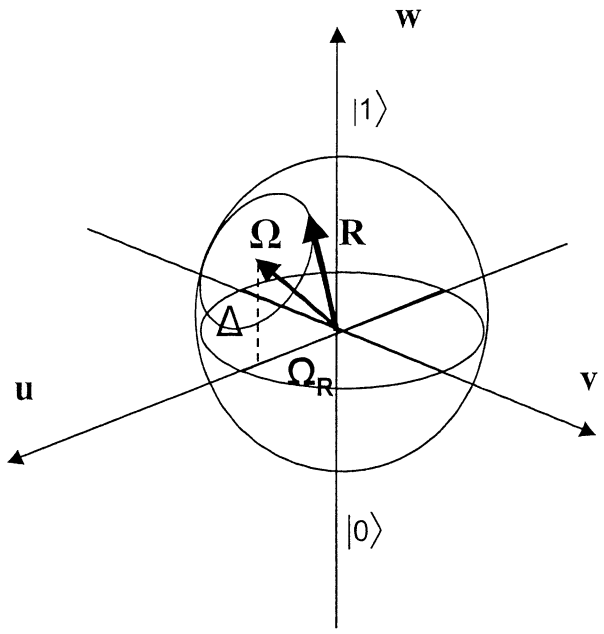

Figure 4. The Bloch sphere. When applying an external field, the Bloch vector, R, starts to process around the vector, Ω, representing the interaction between the atomic system and the field.

3.6 Rectangular pulse with fixed amplitude, frequency and phase

The conditions for a rectangular pulse, with a constant Rabi frequency and no frequency detuning, $\Delta = 0$, is first to be considered. Only the ions that are in exact resonance with the field are affected. The movement is described in the frame of the electro-magnetic field and is essentially described as a change of the v- and w-components. Resolving the equations in (3.5) gives:

$$\begin{aligned} u &= 0 \\ v &= -A\sin(\Omega_R t) + B\cos(\Omega_R t)\,. \\ w &= A\cos(\Omega_R t) + B\sin(\Omega_R t) \end{aligned} \tag{3.12}$$

The population will be oscillating between the ground state 0 and the excited state 1, depending on the so-called pulse area θ:

$$\theta = \Omega_R t\,. \tag{3.13}$$

In order to stop these so-called Rabi oscillations, at the right moment for a desired transition, creating a Rabi-flopping, the laser has to correspond to a definite pulse area. When no interaction between the field and the atoms occurs, at $t = 0$, the atomic population is assumed to be in the ground state. According to the fact the w-component is equal to -1 and the v-component is equal to 0, at t=0, the constant A

corresponds to –1 and B to 0. Therefore, $w = -\cos(\Omega_R t)$ and in order to reverse the population to the upper state and to obtain w equal to 1, the pulse area has to be an odd multiple of π. Pulses with areas equal to even multiples of π, return the system to the initial state, bringing back the value of w = -1. On the other hand, to put an atom in an equal superposition of states, i.e. the rates of the diagonal terms of the density matrix are identical and w=0, a pulse exhibiting a pulse area of an odd multiple of $\pi/2$, has to be applied.

The vector will only move in the (v,w)-plane, since the u-components does not change in time. In other terms, a π-pulse will create a rotation of an angle of 180° on the Bloch-sphere, resulting for a atom starting in its ground state, in a vector that goes from pointing straight downwards to pointing straight upwards. Similarly, applying a $\pi/2$-pulse, causes a 90°-rotation of the Bloch-vector, which corresponds to an even superposition of states, if the atom was in the ground state initially.

However, the sample of ions consists of an ensemble, with a distribution of different transition frequencies. Consequently, in the case of, $\Delta \neq 0$, an additional constraint occur. The duration of the rectangle pulse, t, has to be much inferior to the inverse inhomogeneous width, Δ_0^{-1}, in order to transfer all the non-resonant ions to the excited state. Since the pulse area, θ, has to be equal to π, the following conditions have to be fulfilled for a complete transfer, when a non-zero detuning exist:

$$\left.\begin{aligned} \theta = \pi = \Omega_R t \\ t << \frac{1}{\Delta_0} \end{aligned}\right\} \quad \rightarrow \frac{\Delta_0 \pi}{\Omega_R} << 1. \tag{3.14}$$

By solving the equation in (3.5) with $\Delta \neq 0$, we obtain:

$$\begin{aligned} u &= -\frac{\Delta}{\Omega_R}\left[A\cos(\Omega_R t) + B\sin(\Omega_R t)\right] \\ v &= -\frac{\Omega}{\Omega_R}\left[A\sin(\Omega t) - B\cos(\Omega t)\right] \\ w &= A\cos(\Omega t) + B\sin(\Omega t) \end{aligned} \tag{3.15}$$

The population transfer is very dependent on the Rabi frequency, and satisfying the conditions in Eq. (3.14) is complicated, based on the following factors:

- transverse non-uniformity of the laser beam
- axial attenuation
- non-equivalent sites and the non-uniform orientation of the dipole moment

To simplify the conditions of the inversion of populations, a laser field where the laser frequency is changing can be applied. This is done with a laser pulse, with constant amplitude, but with a frequency varying at a chirp rate, r. The chirp rate, r, is the change in frequency, per units of time.

3.7 Rapid adiabatic passage (RAP)

In producing a total population inversion, a finite pulse area has to be created within the limitations of the inhomogeneous line width. A less severe condition, can be reachable by using a stabilised laser source with a fast chirp rate, r. This technique is called Rapid Adiabatic Passage (RAP). In the following part it will showed how it is possible to drive the Bloch-vector, from a position of aligning straight downwards to a final position of being aligned straight up, by varying the frequency of the applied laser field. By using this method one gets rid of the conditions of producing a pulse exhibiting a pulse area equal to π.

3.7.1 Vectorial picture

The laser, with a varying frequency, operates during the time, t, at a chirp rate, $r = \frac{d\Delta}{dt}$. During the chirp, the pulse will interact with atoms at different transition frequencies. The detuning, $\Delta = rt$, starts from $\Delta = -\infty$ when $t = -\infty$, passes through $\Delta = 0$ and finally it is at $\Delta = +\infty$ when $t = +\infty$. The vector representing the driving field in the Bloch space, undergoes a π rotation around the axis when t varies from $-\infty$ to $+\infty$. The initial fixed-frame equation can be changed into a rotating frame-equation, to better analyse these motions.

The rotating frame is defined in such a way that the v'-coordinate is fixed, remaining aligned with v, while u' is aligned along the rotating vector representing the driving field. In the rotating frame the equation of motion reads as:

$$\left.\frac{d\bar{R}}{dt}\right|_1 = \left.\frac{d\bar{R}}{dt}\right|_0 + \bar{\omega}\times\bar{R}$$
$$\left.\frac{d\bar{R}}{dt}\right|_1 = (\bar{\Omega}+\bar{\omega})\times\bar{R} \qquad (3.16)$$

In the rotating frame the equation of motion keeps the same form as in the fixed frame except that $\bar{\Omega}$ is replaced by $\bar{\Omega}+\bar{\omega}$. If $\omega << \Omega$ the Bloch vector simply precesses around $\bar{\Omega}$ at angular speed Ω. Then, in the fixed frame, the Bloch vector initially precesses around a vector heading downward and finally precesses around a vector pointing upward. This results in coherent population transfer from the ground state to the upper state.

But, what is $\bar{\omega}$ and its restrictions? To solve for $\bar{\omega}$, we introduce $\hat{\Omega}$, expressing the unit vector:

$$\hat{\Omega} = \frac{\bar{\Omega}}{\Omega} = \begin{pmatrix} \frac{-\Omega_R}{\Omega} \\ 0 \\ \frac{\Delta}{\Omega} \end{pmatrix} \qquad (3.17)$$

Then $\hat{\Omega}$ satisfies the change-of-frame equation:

$$\left.\frac{d\hat{\Omega}}{dt}\right|_1 = \left.\frac{d\hat{\Omega}}{dt}\right|_0 + \bar{\omega}\times\hat{\Omega}\,. \tag{3.18}$$

The $\hat{\Omega}$-vector's variation in time in the new frame is equal to 0, which after further developing gives us the following equations that will reveal the amount of $\bar{\omega}$:

$$\bar{\omega} = -\bar{\Omega}\times\left.\frac{d\bar{\Omega}}{dt}\right|_0 \tag{3.19}$$

$$\omega = |\bar{\omega}| = \frac{r\Omega_R}{\Omega^2}\,. \tag{3.20}$$

This frequency, $\bar{\omega}$ has to be much smaller than Ω, resulting in:

$$\Omega^2 << r\Omega_R \tag{3.21}$$

This should be fulfilled at any time, but regarding the minimum value of Ω, i.e. when $\Omega = \Omega_R$, following expression reads as:

$$r >> \Omega_R \tag{3.22}$$

which is the adiabatic transfer conditions. This is an improvement, compared to a π-pulse, because the equality conditions, $\theta = \pi$, are replaced by a threshold condition. Additionally, as in any other coherent process, the operation should be proceeded within less than the atomic coherence lifetime, the rapid transfer passage can be expressed like:

$$\frac{\Omega_R}{r} << \frac{1}{\gamma_{ab}} \tag{3.23}$$

which is the reason why the passage has to be fast. This can be illustrated in the Bloch sphere, where the Bloch vector has to be tilting from a downward position to a straight upward in less than $T_2 = (\pi\gamma_{ab})^{-1}$ to achieve a transfer like that. When Eq. (3.23) is fulfilled, a 100% population transfer can be produced [8]. This makes RAP to be a very convenient and solid technique against variations in the parameters and will facilitate the examination of coherent aspects.

3.7.2 Complex hyperbolic secant (CHS)

This description of rapid adiabatic passage supposes that the driving field interacts with each ion a long time before and after being exactly in resonance with this ion. During this time interval the amplitude of the driving field is supposed to be maintained at a constant value. Experimentally, these conditions are difficult to satisfy. The field is applied to the sample during a limited time. In addition, when the spectral interval covered by the chirped laser is narrower than the transition

frequency distribution, the different ions endure different interaction conditions. Especially the ions located at the edges of the scanned interval interact a short time with the field, either before or after resonance crossing.

Smoother variations of the field are expected to eliminate discontinuities associated with abrupt switch on and off [9]. The complex hyperbolic secant (CHS) pulses apparently combine smooth variations and adiabatic passage conditions. Let the excitation field be shaped in such a way that the Rabi frequency reads as:

$$\Omega_R(t) = \Omega_0 \sec h(\beta(t-t_0))^{1+i\gamma} = \Omega_0 \cosh(\beta(t-t_0))^{-1-i\gamma} \tag{3.24}$$

where γ is a constant and t_0 is the initial time of the pulse. This expression can also be written by:

$$\Omega_R(t) = \frac{\Omega_0}{\cosh(\beta(t-t_0))} e^{i\gamma \ln\cosh(\beta(t-t_0))}. \tag{3.25}$$

The phase factor gives rise to an instantaneous frequency shift that reads as:

$$\nu(t) = \frac{d\varphi}{dt} = \gamma\beta \tanh(\beta(t-t_0)) \tag{3.26}$$

and the chirp rate can be expressed as:

$$r(t) = \frac{d\nu}{dt} = \gamma\beta^2 \frac{1}{\left[\cosh(\beta(t-t_0)\right]^2}. \tag{3.27}$$

One observes that:

$$\frac{\Omega_R^2(t)}{r(t)} = \frac{\Omega_R^2(t_0)}{r(t_0)} = \frac{\Omega_0^2}{\gamma\beta^2} \tag{3.28}$$

Therefore, if the adiabatic passage condition $\Omega_R^2(t) >> r(t)$ is satisfied at time t, it is satisfied at any moment all along the pulse duration. This suggests that, provided $\Omega_0^2 >> \beta^2\gamma$, efficient RAP could take place. According to Eq.(3.30), the spectral interval spanned by the CHS pulse reads as:

$$2\Delta\omega = 2\gamma\beta \tag{3.29}$$

A more refined calculation confirms this intuition. An analytic solution to the Bloch equations with a CHS driving field was presented for the first time by M.S. Silver et al [10], in the NMR context. This solution to the Bloch equations shows to be applicable also to atomic population inversion by an optical field. Solutions are expressed in terms of the hypergeometric function.

We are especially interested in the final population difference, starting with no atomic coherence in the initial state. The $\pm\infty$ time limits refer to initial and final

state respectively. Depending on the relative size of Ω_0 and $\beta\gamma$, two different expressions are obtained:

1. when $\Omega_0 \geq \beta\gamma$

$$\frac{n_{ab}(\Delta, t \to +\infty)}{n_{ab}(\Delta, t \to -\infty)} = \tanh \pi \left(\frac{\Delta}{2\beta} + \frac{\gamma}{2} \right) \tanh \pi \left(\frac{\Delta}{2\beta} - \frac{\gamma}{2} \right)$$
$$+ \cos \left\{ \pi \sqrt{\left(\frac{\Omega_0}{\beta} \right)^2 - \gamma^2} \right\} \operatorname{sech} \left\{ \pi \left[\left(\frac{\Delta}{2\beta} \right) + \frac{\gamma}{2} \right] \right\} \operatorname{sech} \left\{ \pi \left[\left(\frac{\Delta}{2\beta} \right) - \frac{\gamma}{2} \right] \right\} \tag{3.30}$$

2. when $\Omega_0 < \beta\gamma$

$$\frac{n_{ab}(\Delta, t \to +\infty)}{n_{ab}(\Delta, t \to -\infty)} = \tanh \pi \left(\frac{\Delta}{2\beta} + \frac{\gamma}{2} \right) \tanh \pi \left(\frac{\Delta}{2\beta} - \frac{\gamma}{2} \right)$$
$$+ \cosh \left\{ \pi \sqrt{\gamma^2 - \left(\frac{\Omega_0}{\beta} \right)^2} \right\} \operatorname{sech} \left\{ \pi \left[\left(\frac{\Delta}{2\beta} \right) + \frac{\gamma}{2} \right] \right\} \operatorname{sech} \left\{ \pi \left[\left(\frac{\Delta}{2\beta} \right) - \frac{\gamma}{2} \right] \right\} \tag{3.31}$$

It should be noticed that only the first solution, when $\Omega_0 \geq \beta\gamma$, has been considered by M.S. Silver et al [10].

In both expressions the population transfer is mostly efficient when the second term in the right hand side of the equation is much smaller than unity. This condition is satisfied in Eq. (3.31) as soon as $|\Delta| < \beta\gamma$ and $\gamma > 2$. However this solution corresponds to rather large values of the Rabi frequency that is supposed to be larger than the excitation spectral interval.

In Eq.(3.31), the second term on the right hand side can be expressed as:

$$C = 4 \cosh \left\{ \pi \sqrt{\gamma^2 - \left(\frac{\Omega_0}{\beta} \right)^2} \right\} \exp(-\pi\gamma) \tag{3.32}$$

when $|\Delta| < \beta\gamma$ and $\gamma > 2$. Since $\exp(-\pi\gamma) << 1$, upper limit values of C satisfying $C << 1$ will involve large values of $\cosh \left\{ \pi \sqrt{\gamma^2 - \left(\frac{\Omega_0}{\beta} \right)^2} \right\}$. Therefore, in this upper limit region C reads as:

$$C = 2 \exp \left(\pi \sqrt{\gamma^2 - \left(\frac{\Omega_0}{\beta} \right)^2} - \pi\gamma \right)$$
$$= 2 \exp \left(-\pi\Omega_0^2 \Big/ \left[\beta \sqrt{\beta^2\gamma^2 - \Omega_0^2} + \beta^2\gamma \right] \right) \tag{3.33}$$

and the condition for $C << 1$ reads as:

$$\pi\Omega_0^2 >> 2\beta^2\gamma \tag{3.34}$$

which is nothing but the adiabatic passage condition!

4 The experiments

The experiments were carried out on two different Tm^{3+}-doped YAG-crystals, the first one with a Tm^{3+} atomic concentration of 0.5 % and the second one with 0.1 %. One of the crystals has an arbitrary projection of the dipole moments along the electromagnetic field that will be applied. In the other sample all the ions have the same projection of the dipole moment along the applied laser field. The second sample used, has many advantages in comparison to the first one when it comes to achieving a uniform population transfer, mainly thanks to its well-known dipole moment direction and to the reduced optical density, due to a lower ion concentration.

The sample is immersed in a cryostat filled with helium at a temperature of 1.4 K, obtaining a life time of the optical dipole of the Tm^{3+} ions to be around 75μs [11]. The decay rate of the meta-stable state (see Figure 3) is much smaller than the upper level decay rate [12].

A single frequency laser with a frequency stabilisation of $\Delta\nu < 1$ kHz over 10 ms serves as the excitation source. The laser beam is divided into a writing beam and a probing beam with the help of an acousto-optic modulator (AO), which can be studied in Figure 6. This modulator has two functions, it makes all laser light to be transmitted, in the writing step, and no energy will be wasted, and secondly, it is used to scan the frequency in the probe beam. Another AO is used to shape the writing beam in amplitude and phase. Both AO's are adjusted so that they have the same carrier frequency. Two different beams are used in the writing and probing process, because we want to probe only the central region of the exposed area of the sample to assure that all the ions that are probed have experienced the same writing intensity. Thus, the waist size of the writing beam and the probing beam are adjusted independently in such a way that the probe beam size is about half of the writing beam size. The transmitted beam is finally detected with a avalanche photodiode detector (Hamamatsu C5460).

4.2 The acousto-optic modulators

The writing and reading procedure of the applied field has to be made separately, to avoid the writing beam from erasing what has just been engraved, once starting the probing process. In order to control the phase, the amplitude and not to mention the timing of the different beams, a device that separates and modulates the beams is crucial. An acousto-optic modulator is used in order to enable the treatment of one beam at the time.

An acousto-optic modulator is constituted of a crystal, in this case, made of TeO_2 that is fed with a radio frequency signal at the wavelength, Λ. The wave creates a variable refractive index of the crystal, which acts as a diffraction grating. The periodic modulation of the refractive index, results in a splitting of the transmitted laser beam into different diffraction orders that can now be detected and analysed separately. Both reflection- and transmission grating can be created, whereas in

these experiments only a transmission grating is used. If the angle of incidence and the wavelength of the modulation wave are well-adjusted, 100 %of the light can be transmitted in the first diffraction order (m=1). Also the size of the beam is a very important parameter. The size has to fulfil two criteria. On one hand, the focused beam waist, w, has to be inferior to the size of the piezo-optical transducer with the height, d (see Figure 5) that feeds the acoustic waves into the crystal. On the other hand, the size of the beam waist has to be larger than the wavelength, Λ, of the acoustic wave. The reason of this is that, by knowing that the angle of deflection can be expressed by the laser wavelength divided by the acoustic wave length, while the angle of diffraction is the relationship between the laser wave length and the size of the waist, the condition in order to separate the diffraction orders at the exit of the AO, will be that the angle of deflection has to be much superior to the angle of diffraction. Calculations give us the following information: The velocity of the acoustic wave being v = 4200 m/s, the frequency being f = 100 MHz, gives the wavelength of around 40 μm, which will be the minimum diameter of the laser beam waist.

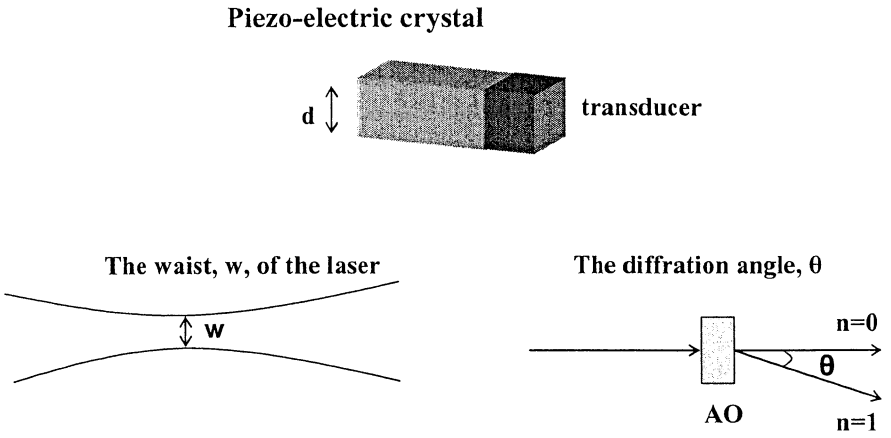

Figure 5.

4.3 Electronics

All the electrical instruments are commanded by a pulse generator of the type Stanford Research DG 535 that has one fixed output and one output with an adjustable delay. The adjustable delay output triggers a wave form generator (Sony-Tektronix AWG 520) that drives the acousto-optic modulators, enabling to shape each beam in amplitude and phase. The sample frequency is 1 GHz, in the carrier frequency generated for the AO modulators that is 80 MHz. The two different out-puts of the AWG 520 generators control the AO modulators separately and are programmable in any desired algebraic modulation envelope.

4.4 The set-up

The experimental setup is drawn in Figure 6. The very first thing is to adjust the shape of the laser spot, from being a bit elliptic to be more circular. This is made by an anamorphic prism-pair (1). A Faraday isolator (2) is then placed in the beam to eliminate reflections on the laser. A small fraction of the laser radiation will be separated from the beam to the laser stabilisation device (5) by an uncoated mirror (4). At the exit of the laser, the electromagnetic field is oscillating horizontally and with the uncoated mirror only around 1 % will be reflected towards the stabilisation device. A half wave plate (3) is therefore used to change the polarization of the light, making at least 10 % of the light to be reflected. The rest of the beam a bit further ahead will be, directed by an identical uncoated mirror, to a λ-meter (Burleigh WA1000) (6), making sure that the laser field is in the middle of the desired wavelength band.

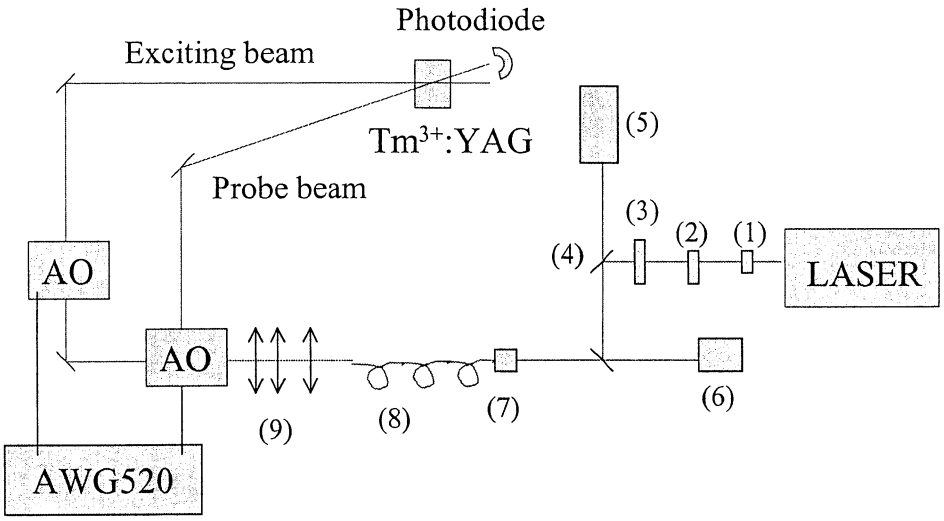

Figure 6. The experimental set-up.

With a microscope objective (7) the field is focused into an optical mono-mode fibre (8). The beam will have an almost Gaussian shape at the end of the fibre, which is a great advantageous when focusing on the sample. Applying a telescope set-up (9) of three different lenses the beam will be reduced, and focused on the first acousto-optic modulator.

The purpose of the first AO is to divide the beam into a writing beam and a probing beam. It is adjusted so that, when the AO is running, the light will be in the first diffraction order, producing the probe beam. When the AO is switched off, all the light will pass straight through the modulator, without being affected, which is the zeroth order and serves as the engraving field. This beam will be modulated once more in a second AO, also called an AO-shifter that is commanded by a waveform generator programmed to shape the field amplitude.

Looking closer on the pulses in terms of writing and probing sequences and the opening and closing of the acousto-optic modulators, a time diagram is illustrated in Figure 7.

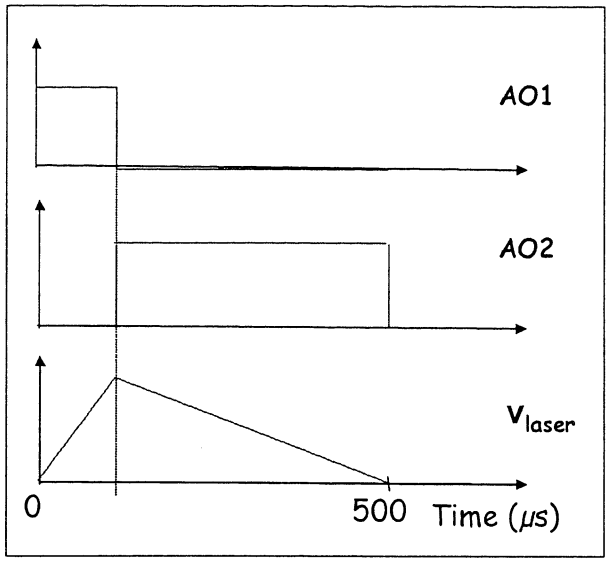

Figure 7. The acousto-optic modulator AO1, is activated during the writing pulse, performing a frequency chirp. In order to protect the crystal from any writing process during the probing, the modulator AO2 is switched, producing a splitting of the laser beam.

The writing and the probe beam are then overlapped again, collimated and focused on the crystal. At the crystal the radius of the writing beam is typically 70 μ m and the probe beam 30 μ m. In order to protect the detector while engraving, the writing beam is eliminated by yet another acousto-optic modulator. The AO will be adjusted to detect the signal in the first diffraction order and letting the excitation beam pass through in the zeroth order, without hitting the mirror that sends the light onto the detector. The signal is finally detected with a avalanche photodiode detector (Hamamatsu C5460).

4.5 The laser

Coherent driving requires a stabilised laser source. In these quantum experiments a laser with a line width narrower than the atomic transition line width, at a few Kelvin is to prefer. Such a laser would be the perfect tool in controlling quantum states.

A semiconductor laser, with an external cavity, is used. The laser is extended in a Littrow configuration (the diffraction order n =+1 is utilised) and has an electro-optical crystal of Lithium Tantalate. The crystal enables a sweep of 50 GHz at a wavelength of 793 nm, without mode hops. It also provides a agility of at least 0.1

GHz/μs. These are very good conditions for experiments in Thulium. However, the homogeneous line width of Thulium is a few kHz at super fluid Helium temperature and the stability of the laser is only 5 MHz over 10 ms, and has to be improved for a coherent driving process in Thulium to be possible. Frequency stabilization of the laser is therefore very essential.

There is an electro-optical crystal in the laser cavity that makes the laser work as a Voltage Controlling Oscillator (VCO). The frequency of that oscillator is controlled via an input voltage that locks the cavity to a desired frequency and in that way is closing the stabilisation loop. Once the loop is closed, the phase will remain fixed and stable, and the laser will be able to rapidly sweep over a narrow frequency interval with the help of an acousto-optic modulator. A simplified scheme of the different elements of the loop is presented in Figure 8. The frequency, ν, corresponding to the cavity, is compared to a reference frequency. The disagreement in frequency, $\Delta\nu$, give raise to a signal that is dealt with in the frequency-to-voltage converter. If there is a detuning, the loop generates a voltage to compensate for this and then the signal is being filtered and amplified before it is fed back to the oscillator.

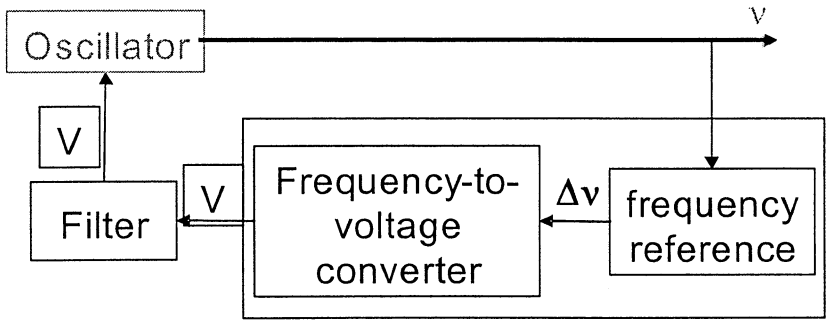

Figure 8. A simplified scheme of the stabilization loop.

This stabilization loop is basically characterized by an external cavity, composed by a high finesse Fabry Perot cavity, in a reflection mode. A Fabry Perot consists of two mirrors separated by a length L, and high finesse means that the mirrors in the cavity have a high reflectivity. The reflection function, $R(\nu)$ depends on the laser frequency, ν. By monitoring the intensity that is reflected off the cavity the laser frequency can be locked to a cavity transmission peak. The resonance frequencies of the cavity are separated by the free spectral width, FSR (= c/2L) and the resonance line width is FSR divided by the cavity finesse. In our set-up, the spectral width is 1.5 GHz and the finesse ($F=\pi R^{1/2}/(1-R)$) is 3000, giving a resonance full width at half maximum (FWHM), $\delta\nu$, of 500 kHz.

Figure 9. The length, L, the free spectral range, FSR and the full width at half maximum (FWHM) of the laser cavity.

The laser is modulated at the modulation frequency f_m, 20 MHz with a RF local oscillator. The modulation creates two sidebands, with two peaks with opposite signs, 20 MHz apart (see Figure 10). The electric field that is reflected and detected, when the laser is not locked can be expressed by:

$$I_R(t) = A + B\cos(2\pi f_m t) + C\sin(2\pi f_m t) + \varepsilon(2f_m) \ . \qquad (4.1)$$

This signal is generated from the three different peaks, at $\nu + f_m$, ν and $\nu - f_m$, and are representing the interference between the optical carrier resonant with the cavity and the modulation bands directly reflected as well as some leakage field from the cavity. The parameters A, B and C are trigonometric functions. When in resonance, both the second and the third term are zero and very close to resonance, the sine term is linearly dependant on the frequency detuning. This linearly dependent window is exactly the cavity resonance bandwidth and it provides an error signal of the laser, with respect to the cavity.

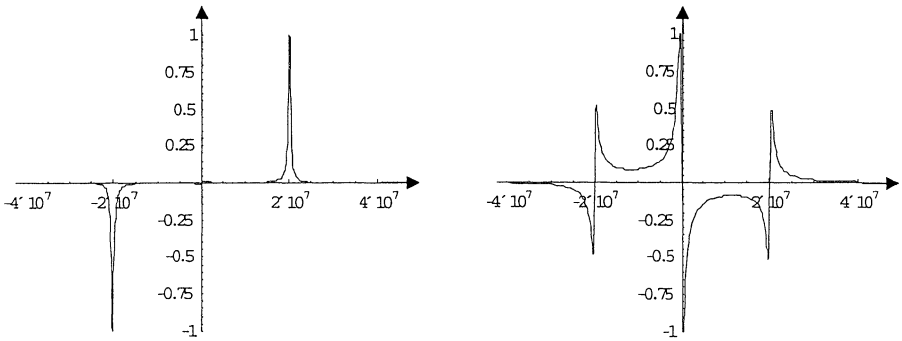

Figure 10. The detected signal, showing the interference between the cavity and the modulation signal, in terms of the intensity as a function of the frequency. The diagram to the left, represents the second term in Eq. (4.1) and the diagram to the right the third term in Eq. (4.1).

In this way a good error signal is selected and the reference cavity can be regarded as a first order low pass filter. After detection, the signal is demodulated with the local oscillator, which is done by the multiplication of the detected signal and the

local oscillator. The error signal is then treated in the filter and finally fed back via the electro-optic crystal to the laser.
One of the greatest advantages with this kind of scheme, is the big modulation width, compared to the resonance at FWHM. When modulating, the resonance line width will be very probable to fall within the same spectrum as the modulation signal and therefore, the cavity is easier to lock. Moreover, this method does not require direct modulation, meaning that the modulation is not done on the laser itself, but in the external locking loop.

Another convenient aspect is that this kind of set up requires low power, and the laser power can be fully used to other parts of the experiments.

In conclusion, the most essential with this type of highly stabilised laser in the experiments on Thulium, is that when the loop is closed the laser reaches a spectral width in the range of kHz, corresponding to a coherence time that is much superior to the life time of the atomic coherence on the scale of the meta-stable state life time. Therefore, the coherent atomic manipulations are proceeding during a time that is a lot shorter than the stabilization time of the laser ($\frac{\Omega_R}{r} << \tau_{laser}$) and it will be possible to control the Thulium population transfer in a coherent way.

5 The results of adiabatic passage

In studying the efficiency of the population transfer, we are measuring the intensity of the laser beam after passing the sample. The writing beam is exciting the ions to the upper level, and shortly thereafter, a non-radiating decay to a third state takes place. This third state has a relatively long life time and is referred to as the meta-stable state or the meta-stable state. In repeating the excitation, within the life time of the meta-stable state, all the ions will be transferred from the ground state, to the third state, via the excited state and the sample is said to be bleached. When the sample is bleached, no further excitation is possible and the material will be transparent to light in that wavelength. This contributes to an important reference in terms of predicting how much of the light that enters will be absorbed in the crystal when no excitation is taking place. This is referred to as the optical density of the material. In general, one can express the exponential decay of a ray of light passing through a material, at the rate of αL, or else as a decay function proportional to 10^{-D}, where D is the optical density, characteristic of the material with thickness, L, as:

$$I = I_0 e^{-\alpha L} \quad \text{or} \quad I = I_0 10^{-D} \tag{5.1}$$

where I_0, corresponds to the light intensity before entering the material. Since the material will be excited of the beam crossing the material, the difference in population rates between the ground state, $N_g(t)$ and the excited level, $N_e(t)$ can be measured. The optical density is therefore multiplied by the difference of the population rates, and with the relation between the parameter, α and D:

$$\alpha L = \ln\left(\frac{I_0}{I}\right) \quad \text{and} \quad D = \log\left(\frac{I_0}{I}\right) \tag{5.2}$$

knowing that:

$$D = \frac{\ln\left(\frac{I_0}{I}\right)}{\ln 10}. \tag{5.3}$$

The decay of the population can be now be developed into:

$$I = I_0 10^{-D(N_g - N_e(t))} \tag{5.4}$$

The population rate, $N_e(t)$ can also be presented in terms of a exponential decay at a rate $-\frac{t}{\tau}$, starting from t=0, corresponding to the moment when the ions are excited. Immediately thereafter the population starts to decay to the meta-stable state with a rate, representing the time, t, between the writing and probing, compared to the life time, τ, of the meta-stable state. The expression reads as:

$$N_e(t) = N_e(0)e^{-t/\tau}. \tag{5.5}$$

In measuring how much of the light that has dispersed only due to the properties of the material, the optical density is obtained by comparing the intensity before and after the sample, when out of resonance with the optical transition frequency, so no transfer is taking place. Knowing this parameter, it will be possible to measure how much of the ions have been excited and how much that already has been relaxed to the meta-stable state, since they will no longer contribute to the transmission profile. Since the sum of the population rates $N_e(0)+N_g(0)$ at the time, t=0, is equal to 1, this will also be the true for a time that is rate of excited ions is calculated from the following expression:

$$N_e(0) = \frac{1+\frac{1}{D}\log(\frac{I}{I_0})}{1+e^{-t/\tau}} \tag{5.6}$$

In choosing an appropriate chirp rate, one has to make sure that the experiments are fulfilling the adiabatic passage conditions. The Rabi frequency is calculated, by using the power, P of the writing beam. The expression of the Rabi frequency is developed into the following:

$$\Omega_R = \frac{\mu_{ab}}{\hbar}\sqrt{\frac{2P_{writing}}{S\varepsilon_0 c}} \tag{5.7}$$

where ε_0 is the permittivity of vacuum, c is the velocity of light and S stands for the surface of the beam ($S = \frac{\pi}{2}10^{-8}m^2$). With a chirp rate of r = $2*10^{10}$ Hz/s, the rate, $\frac{\Omega_R^2}{r}$ gave 7.44, proving that the condition for an adiabatic transfer is satisfied.

5.1 Rectangular pulse with fixed amplitude and varying detuning

In the initial experiments, the aim is to create a population transfer by sweeping the frequency of the laser with fixed amplitude (see Figure 11). The ions have slightly different transition frequencies, making them all in resonance and transferred to the excited state at different times, as the swept laser pulse is applied. At the centre of

the swept pulse the inverted wavelength is $\sigma = 12604.50\ cm^{-1}$, the current on the laser is 64 mA and the power of the writing beam at the crystal is 1.85 mW. Both excitation by a single shot, corresponding to 10 Hz as well as excitation by accumulation, at a repetition of rate 1 kHz, were carried out. During the first measurements chirp rates of $r = 1*10^{10}$ Hz/s and $r = 2*10^{10}$ Hz/s were used. The duration of the probing beam was 400 μs, whereas the writing beam lasted for 75 μs, giving us t = 237.5 μs, which is the time between the centre of the writing pulse and the centre of the probing pulse. The optical density obtained was 0.64. From the obtained results (see Figure 12), it was a clear distinction between a single shot and an accumulated transfer. There is an amplification of the transmitted signal in the single shot, because of the coherent process, whereas the accumulated excitation is not taking place within the coherence lifetime and therefore no amplification is noticed. The obtained rate of population transfer in a single shot was 78%.

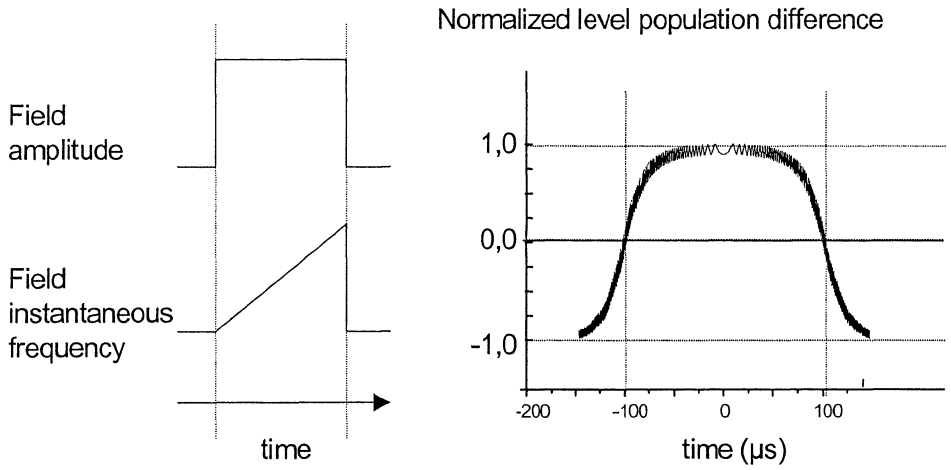

Figure 11. A pulse with constant amplitude and varying detuning was applied (left). The calculated population difference between the upper state and the ground state (right), when applying a pulse shaped as in the graph on the left hand side.

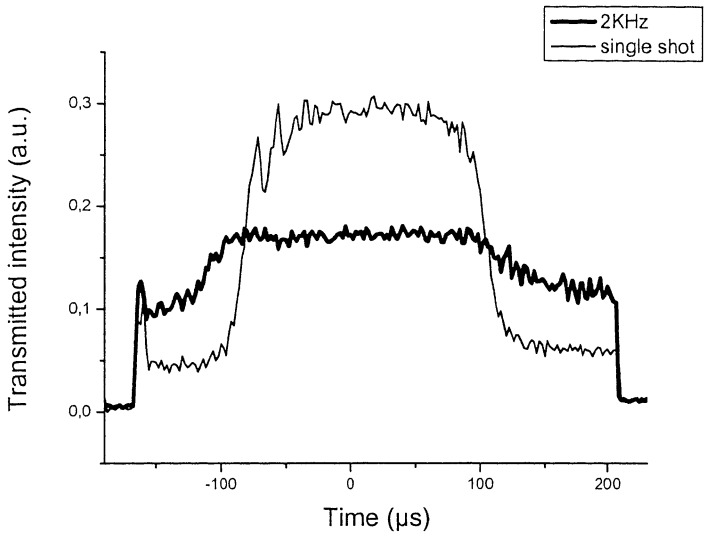

Figure 12. The transmission profile obtained by single shot, respectively accumulation, in adiabatic passage experiments.

5.2 Complex hyperbolic secant pulse (CHS)

Similar experiments as described above are carried out by varying the amplitude and the phase of the applied pulses (see Figure 13). The average of the chirp rate used was $r = 1*10^{10}$ Hz/s, obtained by the duration of the writing beam of 75 μs and a frequency sweep of 750 kHz. The duration of the probe pulse is the same as earlier. We obtained 78 % of population transfer, which is about the same as in the adiabatic passage experiments. Nevertheless, there is an improvement of the shape of the transmission profile and the edges are sharper, since the wings have been remarkably diminished. With the adiabatic transfer, oscillations at the edges are noticed, which is not the case in using a CHS pulse. We also noticed a decrease in transfer efficiency to around 75 %, when using the double the chirp rate, which is exactly what is expected, since fewer ions are excited when we are getting closer to the threshold, $\frac{\Omega_R}{r} << 1$, presented in Eq.(3.26).

The same procedure is carried out on the next sample starting up with an adiabatic transfer with the use of a CHS-pulse. We notice that the population transfer is a lot more efficient in this sample. With $r = 1*10^{10}$ Hz/s and a current of 78.8 mA on the writing beam, we reach a population transfer that is 100% in a single shot transfer. The result of this terrific transfer is shown in Figure 14.

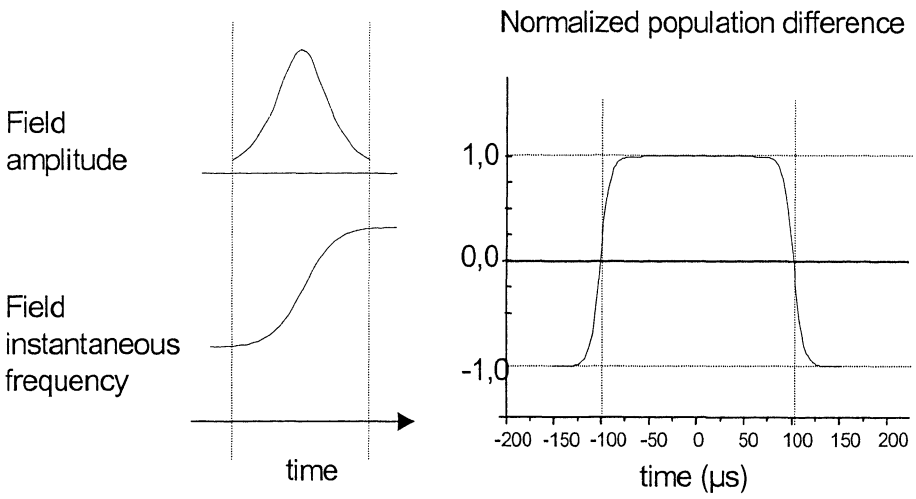

Figure 13. A variation in amplitude and phase is creating a pulse with less oscillations, as can be seen in the theoretical population difference created by this pulse, shown by the diagram on the right hand side.

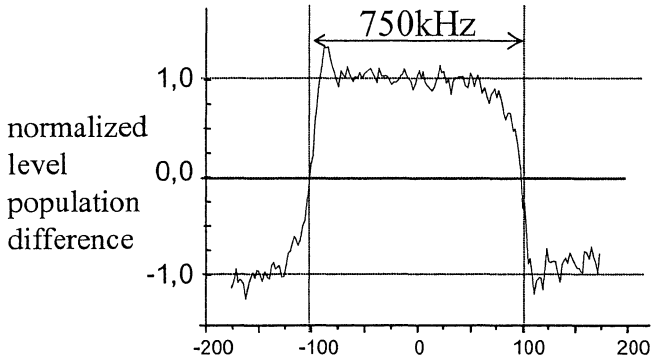

Figure 14. A 100% rate of transfer, produced by a complex hyperbolic secant pulse. There are very little oscillations on the borders of the profile, compared to the profile produced by a constant amplitude and phase.

5.2.1 Study of the transfer at an increasing power of the writing beam

In estimating the transition probability, P, between two states, the Landau-Zener formula [13,14]states that,

$$P = 1 - e^{-(\frac{\pi\Omega_R^2}{2r})}. \qquad (5.8)$$

The probability of transfer should grow exponentially, as the amplitude of the applied field is increased.

This is only true for a constant Rabi frequency and linearly varying detuning. Despite this restriction we will nevertheless be using a complex hyperbolic secant pulse in the following experiments because of the fact that the rate of the Rabi frequency and the varying chirp rate will be constant. In order to examine how population transfer is affected by a change in power of the writing beam, Eq. (5.8) is used producing a varying pulse chirp, with an average chirp rate at $r = 2*10^{10}$ Hz/s and also a varying amplitude of the writing beam varying from 0.1 mW to 1.5 mW. The experiments were made on the second sample, which is the one with lower ion concentration.

An exponential growth of the population transfer could be assumed, until around 0.3 mW, when the sample is being saturated, due to imperfections in the transfer. The fact that the dipole moments are not projected in the same direction on the applied field contributes to the early saturation (see Figure 15).

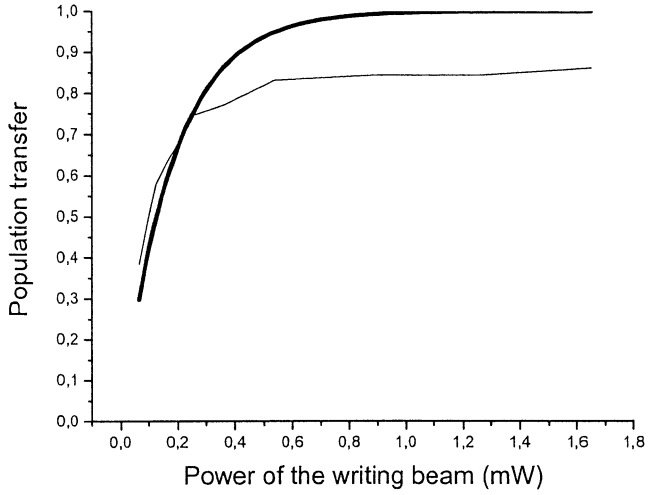

Figure 15. Population transfer as a function of the power of the exciting field, where the thinner line corresponds to the experimental outputs and the thicker line to the calculated values.

5.2.2 Selection of a group of ions and transfer to the excited state and back

In controlling the states of the atoms and their dipole-interaction, it is necessary to select only a minimal range of ions that gain a strong shift in frequency, due to the excitation of neighbouring ions. Having two pure, strongly interacting groups of ions, will make it possible to better study and develop a technique that would bring us closer to the creation of a well-defined quantum state.

Several methods of isolating a single frequency subset of ions have been carried out. Using short laser pulses over a broader frequency range will produce a hole on either side of the chosen frequency and leave a narrow absorption feature. This is called spectral hole burning [4]. Another possibility is producing a rapid adiabatic passage, by applying chirped laser pulses with either fixed amplitude or with an amplitude shaped like a complex hyperbolic secant function.

In experiments, this was first done by applying a rectangular pulse, with not very convincing results, while the use of a CHS pulse showed more promising results. When experiments were done with a CHS pulse on the first and also the thicker sample, only 12 % of the ions affected by the power-dip in the writing field seemed to be possible to isolate in the ground state. But after having prepared the group, it was transferred by 97.4 % from the ground state to the excited state, which is a remarkable good efficiency. The low concentration of ions that are left in the ground state makes the optical density very weak, and this is an advantage for adiabatic passage. Experiments were also done with a third pulse, in trying to inverse the hole, yet another time. This resulted in a transfer rate of 70 %.

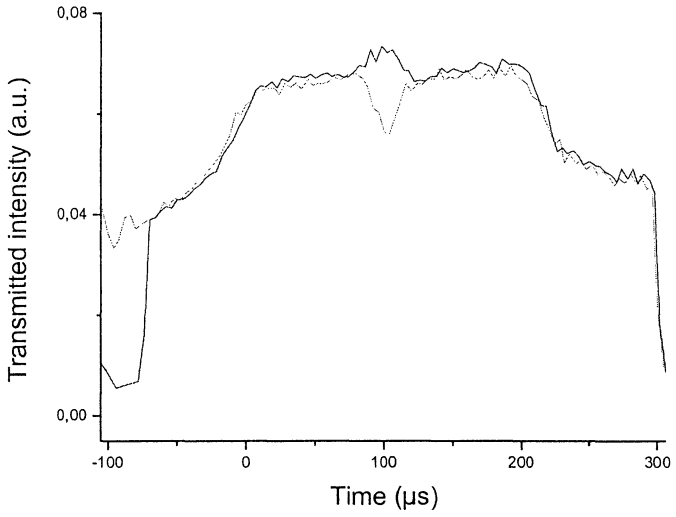

Figure 16. Result of selecting a small group of ions at accumulation and its inversion to the excited state.

To prepare the same characteristic group in the ground state in the second sample is showing better results. Since the dipole moments have a well known direction along with the field, it is easier by one single shot to address more exactly the ions in question. The transmission profile tells us that, almost 88% of the ions that was desired to be immune against excitation, stayed in the ground state and the total amount of ions are excited at an efficiency of 97 %. Notably only 12% were excited. After 5 pulses, a saturation of the total amount of ions is obtained, where now 25% of the ions isolated in the ground state has been excited to the meta-stable level and 75% is left in the initial state. Trying to create an inversion of these ions seems to be harder than in the first sample. Only a rate of 79% is inversed. This is probably because of a higher optical density in this sample compared to the first one, which decrease the efficiency of the adiabatic transfer. Figure 16 shows both the creation of a hole at a repeated transfer and the inversion of it in one single shot.

5.2.3 Laser stabilization

In our interest lies also to examine how big a role the stabilised laser plays in this kind of experiments. To ensure efficient coherent driving, it is necessary to have a

laser with an active stabilisation producing a laser width smaller than the homogeneous width of the ions to be excited. When using a free running laser; the laser jitter is about 5 MHz, which is much larger than the homogeneous width of the Tm^{3+} ions. In Figure 17 the weak performance of population inversion, due to a non-stabilised laser, is confirmed. The time during the transfer is taking place has to be shorter than the coherence time of the laser and also shorter to the coherence time to the ions. The latter condition is fulfilled in this case. Hardly any amplification of the probing beam can be distinguished and the shape of the transmitted field has no longer the same shape as the pulses applied. The single shot will here be very close to the accumulated transfer, since no coherent driving is taking place and only a maximum of 50% in population transfer is reachable.

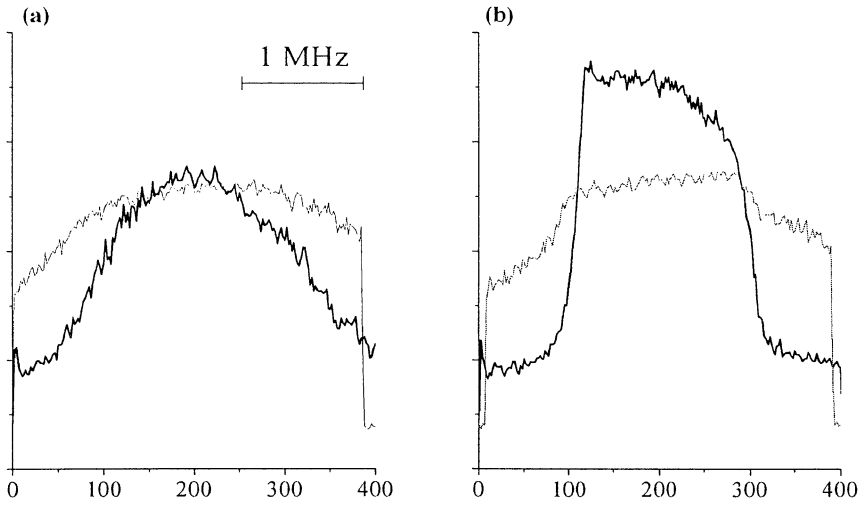

Figure 17. A laser without stabilisation (left) and with stabilisation (right). The thicker line is an adiabatic transfer at single shot and the weaker line is at accumulation.

The affect of stabilisation is very visible also in preparing a narrow ion group, since a fluctuating laser source will widen the expected absorption line and makes it become shallower, whereas the locking of the frequency shows a sharp hole in the transmission feature.

5.2.4 Successive pulses

In the next attempts, we would like to study the excited ions affected by a second pulse that brings them back to the ground state. Ideally, after the second pulse the transmission profile should not show any amplification, since they are brought back in the initial state. Two identical pulses with the duration of 75 μs, right after each other are applied.

Since the first pulse will not create a perfect inversion of population, the transfer will be less efficient, especially on the borders. This defect leaves some rests of ions in the edges of the profile. Nevertheless, in the centre, 75 % of the excited ions was returned to the ground state after the second pulse

The results above was obtained using the sample with an arbitry distribution of the dipole moments, whereas in the other sample these features are more remarkable and are shown in Figure 18. Here, the single shot is showing an exponential decay, very close to the theoretical one, calculated from Eq.(5.5) with t= 237.5 μs and τ = 500 μs. The relaxation can also be interpreted from the form of the peaks on the borders of the ideally flat transmission profile, since the first peak is significantly higher than the second one. Meanwhile, the profile resulting from the accumulated transfer stays stable and shows to be unaffected despite the relaxation, which is exactly corresponding to the theory. The accumulated transfer is saturated, i.e. transferred to the meta-stable state and do not give rise to any relaxation within this short period of time.

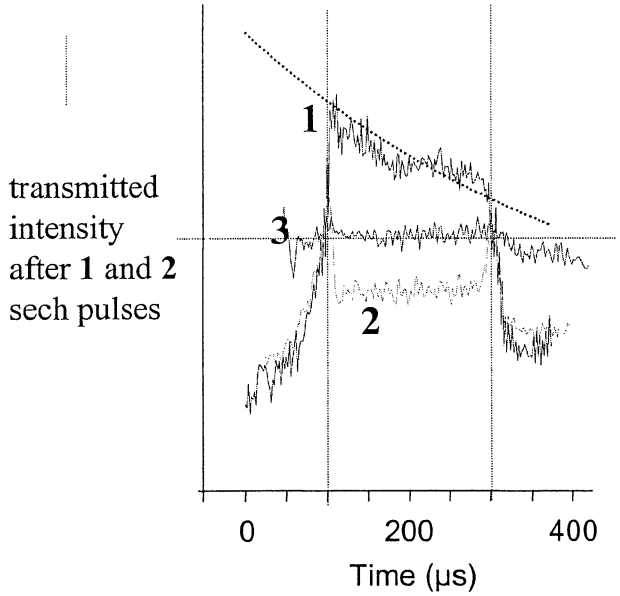

Figure 18. Transmission line shapes acquired after a single shot (1), after a pulse that brings the ions back to the ground state (2) and after accumulation (3), when all the ions have been transferred to the meta-stable state.

With the second sample, the decay was not only studied for two pulses in a row, but the experiments proceeded with three successive pulses, each 75 μs long. Calculations were once again made from Eq.(5.6), giving the difference between the rate of the population in the excited state and in the ground state.

After one single pulse, at the time, t, between the centre of the reading and the centre of the writing (t = 237.5 μs), the theoretical difference, between how much is excited and how much that is still in the initial state, is expected to be 0.62. Thanks to a 100%-transfer, the experimental value was equal to the theoretical one. The writing by two pulses, resulted in a rate of 0.45 and the last reading attempted resulted in 0.37. These experiments have only been carried through once, and the results have not yet been fully analysed. Population transfers with successive pulses will be more thoroughly investigated in the near future.

6 Conclusion

The difficulties from earlier experiments in creating an ideal rapid adiabatic passage, due to the non-uniformity of the laser beam as traversing the sample, as well as power attenuation along the axis, had partly its origins in an inconvenient thickness and concentration of the used sample. By using a new, thinner crystal with a lower concentration and with a well-known direction of the dipole moments, and by changing from a rectangular pulse form to a complex hyperbolic secant shaped pulse, the results with a transfer very close to 100 % have proved the efficiency and robustness of rapid adiabatic passage. The selection of a spectrally narrow ion group by accumulated transfer processes has also been improved and when producing different transfers, with one, two and three successive pulses, the analysis from the experiments, presents a promising continuation of the treatment of rare-earth ions doped material, for the creation of well-defined quantum states. The work described here has also shown how essential it is to have a stabilised laser with a spectral width of sub-kHz, in order to carry out this type of experiments.

Despite many attempts and interpretations, the creation of an isolated ion group, totally immune from excitation, is still not reachable at the extent as desired and the inversion of it can essentially still be improved. Nonetheless, the main objective, which was to transfer all the ions prepared in the ground state to the excited state by coherently manipulating the Bloch vector, has been very successful. Consequently, this leads us to the next step, which eventually will be to prove that the efficient transfer we have obtained is applicable on ions existing in any possible superposition state, which is one of the crucial processes in quantum controlling.

Acknowledgements

Most of all, I would like to thank my supervisor Jean-Louis Le Gouët, for his invaluable help and patience. I would especially like to thank Frédéric de Sèze, and also the others in the group at Laboratoire Aimé Cotton where the work took place; Fabien Bretenaker, Vincent Croazatier, Vincent Lavielle, and Ivan Lorgeré, for all their help and encouragement.

I am also very grateful to Stefan Kröll, for giving me the opportunity to carry out my diploma work in Paris and for introducing me to this project within the fascinating field of optics and quantum computing.

7 References

1. C. A. Sackett et al., Nature **404**, p. 256 (2000).
2. N. A. Gershenfeld, I. L. Chuang; Science **276**, p. 350 (1997).
3. N. Ohlsson, R. K. Mohan, S. Kröll, Opt. Commun. **201,** p. 71 (2002).
4. M. Nilsson, L. Rippe, N. Ohlsson, T Christiansson, S. Kröll, Physica Scripta T **102,** p. 178 (2002).
5. Y. Sun, C. W. Thiel, R. L. Cone, R.W. Equall, R. L. Hutcheson, J. Lumin. **98**, p. 28 (2002).
6. V.S. Malinovsky and J.L. Krause. Eur. Phys. **14,** p. 147 (2001).
7. J. J. Longdell, M.J. Sellars, arXiv:quant-ph/0208182.
8. N. V. Vitanov, B. M. Garraway, Phys. Rev. **53**, p.4288 (1996).
9. N.V. Vitanov, T. Halfmann, B.W. Shore and K. Bergmann. Annu. Rev. Phys. Chem. **52,** p. 763 (2001).
10. M. S. Silver, R. S. Joseph, Phys. Rev. **31,** p. 30 (1985).
11. R. M. Macfarlane, Opt. Lett. **18**, p. 1958 (1993).
12. F. de Sèze, V. Lavielle, I. Lorgeré, J.-L. Le Gouët, Opt. Commun. **223,** p.
13. L. D. Landau, Phys. Z. Sowjetunion **2**, p.46 (1932).
14. C. Zener, Proc. R. Soc.London Ser. **137,** p. 137 (1932).